EBioMedicine 8 (2016) 83–95

Contents lists available at ScienceDirect

EBioMedicine

journal homepage: www.ebiomedicine.com

Research Paper

Functional Rescue of Dopaminergic Neuron Loss in Parkinson's Disease Mice After Transplantation of Hematopoietic Stem and Progenitor Cells

Wassim Altarche-Xifro [a,b], Umberto di Vicino [a,b], Maria Isabel Muñoz-Martin [a,b], Analía Bortolozzi [c,d], Jordi Bové [e], Miquel Vila [e,f,g], Maria Pia Cosma [a,b,g,*]

[a] Centre for Genomic Regulation (CRG), The Barcelona Institute of Science and Technology, Dr. Aiguader 88, Barcelona 08003, Spain
[b] Universitat Pompeu Fabra (UPF), Dr Aiguader 88, 08003 Barcelona, Spain
[c] Institut d'Investigacions Biomèdiques August Pi i Sunyer (IDIBAPS) and Centro de Investigación Biomédica en Red de Salud Mental (CIBERSAM), Barcelona, Spain
[d] Department of Neurochemistry and Neuropharmacology, IIBB-CSIC (Consejo Superior de Investigaciones Científicas), Barcelona, Spain
[e] Neurodegenerative Diseases Research Group, Vall d'Hebron Research Institute and Centre for Networked Biomedical Research on Neurodegenerative Diseases (CIBERNED), Barcelona, Spain
[f] Department of Biochemistry and Molecular Biology, Autonomous University of Barcelona (UAB), Barcelona, Spain
[g] Institució Catalana de Recerca i Estudis Avançats (ICREA), 08010 Barcelona, Spain

ARTICLE INFO

Article history:
Received 6 April 2016
Accepted 14 April 2016
Available online 19 April 2016

Keywords:
Neurodegenerative disorder
Parkinson's disease
Hematopoietic stem and progenitor cells
Cell fusion
Astroglia
Wnt/β-catenin
Intracerebral transplantation

ABSTRACT

Parkinson's disease is a common neurodegenerative disorder, which is due to the loss of dopaminergic neurons in the substantia nigra pars compacta (SNpc) and for which no definitive cure is currently available. Cellular functions in mouse and human tissues can be restored after fusion of bone marrow (BM)-derived cells with a variety of somatic cells. Here, after transplantation of hematopoietic stem and progenitor cells (HSPCs) in the SNpc of two different mouse models of Parkinson's disease, we significantly ameliorated the dopaminergic neuron loss and function. We show fusion of transplanted HSPCs with neurons and with glial cells in the ventral midbrain of Parkinson's disease mice. Interestingly, the hybrids can undergo reprogramming *in vivo* and survived up to 4 weeks after transplantation, while acquiring features of mature astroglia. These newly generated astroglia produced Wnt1 and were essential for functional rescue of the dopaminergic neurons. Our data suggest that glial-derived hybrids produced upon fusion of transplanted HSPCs in the SNpc can rescue the Parkinson's disease phenotype *via* a niche-mediated effect, and can be exploited as an efficient cell-therapy approach.

1. Introduction

Cellular plasticity in mouse and human tissues can be modulated after fusion of bone marrow (BM)-derived cells with a variety of cells, such as neurons, hepatocytes, cardiomyocytes, and gut cells (Nygren et al., 2004; Doyonnas et al., 2004; Ogle et al., 2005; Johansson et al., 2008; de Jong et al., 2012). The hybrids produced can repair the function of these different cell types in a damaged organ (Wang et al., 2003; Johansson et al., 2008; Sanges et al., 2013).

Parkinson's disease (PD) is one of the most common neurodegenerative disorders, and it affects about 1% of the population above the age of 60 years (de Rijk et al., 1997). PD develops due to the loss of dopaminergic neurons in the substantia nigra pars compacta (SNpc), with the consequent degeneration of tyrosine-hydroxylase fibers in the striatum (CPu, caudate-putamen), and dopamine (DA) depletion (de Rijk et al., 1997). No definitive cure is currently available for PD.

We aimed here to determine whether transplantation of hematopoietic stem and progenitor cells (HSPCs) in two different PD mouse models can rescue the loss of dopaminergic neurons after fusion. HSPCs are currently used in clinical-trial protocols (Chen et al., 2014a, 2014b; Park et al., 2015), which suggests their safety.

The neurotoxin 1-methyl-4-phenyl-1, 2,3,6-tetrahydropyridine (MPTP) can induce parkinsonian syndrome in humans that is almost indistinguishable from PD. This treatment produces a dramatic bilateral degeneration of tyrosine-hydroxylase-positive (TH+) neurons in the SN, and of TH+ fibers in the striatum (Bové and Perier, 2012). The neurotoxin 6-hydroxydopamine (6OHDA) triggers death of dopaminergic neurons when injected directly into the brain. Unilateral 6OHDA-injection has also been described as a 'hemiparkinson model', whereby the intact hemisphere serves as the internal control for the resulting asymmetric and quantifiable motor behavior impairment (Bové and Perier, 2012).

Cell therapy of PD is currently pursed in the striatum, through the increase of DA levels (Meyer et al., 2010). Here, however, we transplanted HSPCs into the SNpc of both MPTP and 6OHDA mouse models, with the aim being to regenerate or protect the loss of dopaminergic neurons.

We show that transplanted HSPCs can fuse with neurons and glial cells in both PD models. The glial-derived hybrids survive over the

* Corresponding author at: Centre for Genomic Regulation (CRG), The Barcelona Institute of Science and Technology, Dr. Aiguader 88, Barcelona 08003, Spain.
E-mail address: pia.cosma@crg.es (M.P. Cosma).

http://dx.doi.org/10.1016/j.ebiom.2016.04.016

long-term after the transplantation, and they acquire features of mature astroglia and secrete Wnt1. A niche-effect was associated with an important attenuation of dopaminergic neuronal degeneration. As a consequence, functional amelioration of the PD phenotype was observed. The activity of the Wnt signaling pathway was required for this phenotype rescue.

2. Materials and Methods

2.1. Mice

The mice were housed in accordance with the Ethical Committee for Animal Experimentation of the Government of Catalonia, and the experiments were performed in accordance with the rules set by the local Animal Ethics Committee. ARRIVE (Animal Research: Reporting of *In Vivo* Experiments) guidelines (Kilkenny et al., 2010) were followed.

All of the mice in this study were generated in a wild-type C57BL/6J background. Here, we used wild-type C57BL/6J and the following transgenic mice: CAG-Cre (Hayashi and McMahon, 2002), β-actin-Cre (Srinivas et al., 2001), CAG-RFP (Long et al., 2005), GFAP-Cre (Gregorian et al., 2009), FoxA2-Cre (Park et al., 2008), R26Y (Srinivas et al., 2001), and ROSA26iDTR (Buch et al., 2005a, 2005b).

2.2. Establishment of the MPTP/6OHDA Mouse Models

For the 1-methyl-4-phenyl-1, 2,3,6-tetrahydropyridine (MPTP) mouse model, 8- to 12-week-old male mice received one intraperitoneal injection of MPTP-HCl per day (30 mg/kg free base; Sigma) for five consecutive days, according to the sub-acute MPTP injection paradigm (Vila et al., 2001). Control mice received 0.9% sterile saline injections only. For the 6-hydroxydopamine (6OHDA) mouse model, either male or female mice had 6OHDA injected into the right substantia nigra (SNpc) pars compacta (Parish et al., 2001), under anesthesia and analgesia (2% isoflurane in 2:1 oxygen/nitrous oxide), using a Kopf stereotaxic frame (Kopf Instruments) and a 5 μl Hamilton syringe fitted with a fine capillary. The 6OHDA was used at 1.5 μg/μl (calculated as the free base; Sigma) dissolved in a solution of 0.2 mg/ml ascorbic acid in 0.9% sterile saline. A single injection of 2 μl was performed using the stereotaxic coordinates according to Paxinos and Franklin (2008): −3.0 mm anterior/posterior, 1.05 mm lateral with respect to the bregma, and −4.7 mm ventral from the dura, with a flat skull position. Injections were made at a rate of 0.25 μl/min with a further 4 min allowed for the toxin to diffuse before slow withdrawal of the capillary, followed by cleaning and suturing of the wound. For all *in vivo* experiments, animals were randomized into cages by the animal facility staff, so that the investigator did not select groups based on size or appearance. Establishment of Parkinson's disease model (MPTP and 6OHDA) and the subsequent treatments received were randomly applied on the animals in each cage. Additionally, experiments with mortality rate over 50% after MPTP intoxication were discarded. The sole exclusion criterion was death of the subject animal (due to complications linked with the surgical procedure).

2.3. Cell Preparation and Transplantation

Just before the transplantation, lineage-negative HSPCs were isolated from the total bone marrow of donor mice using Lineage Cell Depletion kits (Miltenyi Biotech). At day 3 after the last MPTP injection or the 6OHDA infusion, the recipient mice were placed into a Kopf stereotaxic frame and received one injection of approximately 60,000 cells suspended in 2 μl phosphate-buffered saline (PBS) over the right substantia nigra (stereotaxic coordinates were determined according to Paxinos and Franklin (2008): −2.9 mm anterior, 1.3 mm lateral with respect to the bregma, and −4.5 mm ventral from the dura, with a flat skull position. The intracerebral injection was performed using a 5 μl Hamilton microsyringe coupled with a 33-gauge needle. Cell infusions were performed at a rate of 0.5 μl/min. On completion of the injection, the needle was left in place for 4 min before being retracted slowly at a rate of 1 mm/min, to avoid reflux along the injection track. After the surgery, the mice were placed under a warm lamp until their complete awakening. To block the Wnt/β-catenin signaling by infusion of Dckkopf-1 (Dkk1) into the SNpc *in vivo*, the recombinant Dkk1 protein (R&D Systems, MN, USA) was dissolved in sterile physiological saline (0.9% NaCl) at a final concentration of 1 μg/μl. One infusion of Dkk1 was carried out unilaterally into the SNpc using a 5 μl Hamilton microsyringe and 2 μg/infusion at the same time of the cell transplantation.

2.4. Tamoxifen Treatment for Cre-recombinase Induction and Diphtheria Toxin Injection

To induce Cre recombination for the YFP labeling, 20 mg tamoxifen (T5648, Sigma) was dissolved in 100 μl ethanol and 900 μl corn oil at 56 °C for 2–3 hours. Tamoxifen was stored in the dark at 4 °C until use, for up to 3 weeks. Tamoxifen was warmed to 37 °C before administration. The mice received intraperitoneal injections of a total 75 mg tamoxifen/kg body weight, once per day for three consecutive days. To ablate the hybrid cells, ROSA26iDTR transgenic mice were injected intraperitoneally with 525 ng diphtheria toxin (D0564, Sigma-Aldrich, St. Louis, MO, USA) in 300 ml PBS per injection, for four consecutive days.

2.5. Neurochemical Analysis

Tissue DA, DOAPC and HVA content were determined on tissue samples from striatum (CPu, caudate-putamen) and cortex (Ctx) by HPLC with electrochemical detection (Waters model 2465; +0.7 V) as previously described (Bortolozzi and Artigas, 2003). Mice were killed and their brains were quickly removed and placed over a cold plate. Caudate putamen (CPu) and cortex were carefully dissected out, weight, frozen on dry ice and kept at −80 °C until assayed. The tissue were homogenized in 200 μl of buffer containing 0.4 M perchloric acid containing 0.1% sodium metabisulphite, 0.01% EDTA, 0.1% cysteine and centrifuged at 12,000 *g* for 30 min. Aliquots of supernatants were then filtered through 0.45 μm filters (Millex, Barcelona, Spain) and analyzed by HPLC as described. The mobile phase consisted of 0.1 M KH_2PO_4, 1 mM octyl sodium sulphate, 0.1 mM EDTA (pH 2.65) and 18% methanol. DA and their metabolites were separated on a Mediterranea Sea (C18, 3 μm, 10 cm × 6.4 mm) (Teknokroma, ref TR010042, Barcelona, Spain).

2.6. Animal Behavior Studies

The motor responses to sensory stimuli in the MPTP-treated mice were measured using the adhesive removal test. Two training trials were performed prior to the surgery, with an adhesive dot sticker (0.6 cm diameter, Avery) placed on the plantar surface of the forelimb. At 4 weeks after Sham or HSPC transplantation of the MPTP-treated mice, the adhesive dot sticker was placed on the forelimb, and the time to make contact and to remove the sticker from the forelimb was recorded. If a mouse did not remove the sticker within 60 seconds (s), it received a score of 60 s. The mean data were calculated across three trials, at one per day. Immediately after this test, the spontaneous activity test was run in the cylinder, by placing the mice into a small transparent cylinder (height, 15.5 cm; diameter, 12.7 cm). The spontaneous activity was videotaped for 3 minutes, and the number of rears and the time spent grooming were measured. To test forepaw akinesia in the 6OHDA mouse model, lesioned mice were randomly assigned to each treatment group, as the Saline group, the control group (6OHDA + Sham), and the group for the transplantation of the HSPCs. To test the spontaneous use of the forelimbs, the cylinder test was

applied to the mice from 4 weeks to 8 weeks after the transplantation. The mice were videotaped in the glass cylinder for 3 min, in the light. The cylinder was placed on a piece of glass and a mirror was positioned at an angle beneath the cylinder to allow a clear view of the motor movements along the ground as well as along the walls of the cylinder. The number of contacts during rearing (measured as the number of supporting touches performed against the cylinder wall) was counted for each paw. The data were presented as the percentage of contralateral paw use over the total contacts. The accelerating rotarod test was used to evaluate the locomotor ability of the mice following MPTP, as described previously (Keshet et al., 2007).

2.7. Unbiased Stereological Cell Counting and Optical Density Measurements

Blinded observers performed all of the assessments. Immunohistochemical staining of the midbrain was examined ($n = 12$ sections/animal) using an optical microscope (Leica, France) equipped with the CAST semiautomatic stereological software (VisioPharm). Then, the total numbers of neurons stained for tyrosine-hydroxylase (TH) and Nissl in the substantia nigra (SN) were counted stereologically. TH+ neuron fibers in the striatum were analyzed according to optical density measurements ($n = 6$ sections/animal). The Image J processing software (National Institutes of Health) was used to analyze the images. These were thresholded to limit measurements to the TH+ fibers, and then an integrated density measurement was obtained by multiplying the TH-stained area by the mean pixel intensity. The TH neuron counts and the optical density of their fibers are expressed as means ± s.e.m. of the percentages of the TH+ cell counts and fibers of the saline controls.

2.8. Quantification and Statistical Analysis

A confocal laser-scanning microscope (Leica TCS-SP5) was used to quantify the immunopositive cells in the sections. All of the quantification of the immunostaining was based on analysis of at least five sections per mouse, from at least three mice. Serial coronal brain sections in the region between −2.06 mm and −3.88 mm from the bregma (Paxinos and Franklin, 2008) (Fig. S1a) were selected and used to quantify the stained areas. The incidence of YFP-immunopositive cells was expressed either relative to the DAPI-stained nuclei (series of sections of the midbrain) or to the number of RFP+ cells for the reporter mice. The data are expressed as means ± s.e.m. of the number of tests stated. Statistical comparisons were made using either Student's *t*-tests for two independent samples or analysis of variance by one-way ANOVA followed by Bonferroni's multiple comparison *post-hoc* tests, as indicated in the Figure legends. All of the statistical tests and graphical presentations were performed using the Prism 5.0 software (GraphPad, San Diego, *CA*). $P < 0.05$ was taken as statistically significant. The distribution and variance were normal and similar in all groups statistically compared.

2.9. Other Experimental Procedures

Other experimental procedures are described in the Supplementary experimental procedures. These include immunofluorescence and histological analysis, FACS analysis, quantitative real time RT-PCR, microarray analysis, and Western blotting.

3. Results

3.1. Transplantation of HSPCs Above the SNpc Ameliorates Dopaminergic Neuron Loss and Function

We have previously shown that transplantation of HSPCs can rescue mouse retinal degeneration (Sanges et al., 2013). The aim here was to determine whether HSPCs can rescue the PD phenotype after their transplantation into the midbrain of the MPTP and 6OHDA mouse models. Thus HSPCs purified from donor mice were unilaterally transplanted above the right SNpc (Fig. 1a).

MPTP and 6OHDA treatments can produce a broad range of mild to severe motor alterations in mice (Meredith and Kang, 2006). In the MPTP model, we examined sensorimotor deficits using the adhesive removal test and the cylinder test (Fleming et al., 2013). In MPTP-treated mice transplanted with HSPCs, the removal time was significantly less in comparison to sham mice (Fig. 1b). In addition, in the cylinder test, there was significantly higher spontaneous activity in the group of HSPC-transplanted mice, with respect to the saline group (Fig. 1b). The rotaroad test is generally used when large doses of MPTP are administered (Duty and Jenner, 2011), a condition different from the sub-acute regimen of MPTP used in the present study. Nevertheless, we observed motor function recovery in the rotarod test in the group of HSPC-transplanted mice 14 days after transplantation. However, no significant differences were seen between the Sham and HSPC-transplanted mice at 28 days after transplantation, due to the behavioral recovery of the Sham group (Fig. S1a).

Using an unbiased stereology system, we then quantified the number of TH-immunoreactive cells in the SNpc and the density of TH+ fibers in the striatum, by optical densitometry. Representative immunohistochemical images showed attenuation of DA neuron degeneration after HSPC transplantation (Fig. 1c; compare Saline, Sham, HSPC groups). Four weeks after transplantation, the percentage of TH+ cells in the sham-transplanted MPTP-lesioned mice remained very low bilaterally, with up to a 42.55 ± 5.36% loss of DA neurons and up to 46.19 ± 4.96% loss of fibers, in comparison with saline-treated animals (Fig. 1d). Interestingly, in the group of HSPC-transplanted MPTP-lesioned mice, the loss of TH+ cells in the SNpc was only around 20.19 ± 4.24%, and the density of TH+ fibers in the striatum was around 26.72 ± 1.86%, compared to saline-treated animals. Thus, there was significant reduction in MPTP-induced loss of dopaminergic neurons in HSPC-transplanted mice (Fig. 1d). As a control, we transplanted lineage+ (Lin+) cells purified from the BM of donor mice, and we observed that the reduction in dopaminergic neurons was comparable in the Lin+ and Sham-transplanted mice (Fig. S1b, c).

We then carried out biochemical measures of the levels of DA and its metabolites in the striatum (Caudate-putamen; CPu) and cortex (Ctx) of HSPC-transplanted mice and controls. There was depletion of CPu and Ctx DA and of the 3.4-dihydroxyphenylacetic acid (DOPAC) and homovanillic acid (HVA) DA metabolites after MPTP administration, with the HSPC-transplanted mice showing a trend toward amelioration in terms of DA in both the CPu and Ctx, and DOPAC and HVA in the Ctx (Fig. S1d). Interestingly, 4 weeks after transplantation, in the MPTP + HSPC transplanted mice the metabolite to DA ratio (HVA/DA), a parameter associated to DA turnover in dopaminergic terminals (Decressac et al., 2012), was significantly lower with respect to the MPTP + Sham mice, in both the CPu and Ctx (Fig. 1e). Furthermore, the DOPAC/DA ratio was also significantly diminished in the CPu of HSPC-transplanted mice (Fig. 1e). These data suggest that DA synthesis and storage was increased after HSPC transplantation in both the striatum and Ctx.

Studies have reported that 6OHDA-lesioned mice show behavioral impairments more clearly (Schallert et al., 2000; Meredith and Kang, 2006); in addition, the intact side serves as the internal control for the lesioned side and its responsiveness to HSPC transplantation. Therefore, we monitored forepaw akinesia of 6OHDA-lesioned mice from 4 to 8 weeks after HSPC transplantation, using the cylinder test. In line with previous studies, 6OHDA lesion reduced the use of the contralateral paw (Schallert et al., 2000). Intracerebral HSPC transplantation restored this deficiency in the grafted mice, an effect that remained significant up to at least 4 weeks (Fig. 1f).

The 6OHDA injections resulted in a loss of DA cells down to 41.08 ± 9.00% of control levels and a loss of fibers down to 46.66 ± 12.58%

(Fig. 1g, h; compare Saline, Sham, HSPC groups). The Saline group was the contralateral, left hemisphere side (Fig. 1g, LH), which was not injected with 6OHDA. Interestingly, the 6OHDA effects were ameliorated by intracerebral HSPC transplantation, which successfully prevented 6OHDA-induced neurodegeneration of DA cells (DA cells, 23.44 ± 5.05% loss of control levels; fibers, 26.25% ± 9.29% loss of control levels; with no statistically significant difference with respect to the Saline group) (Fig. 1h). These data obtained for the 6OHDA mice, as with those

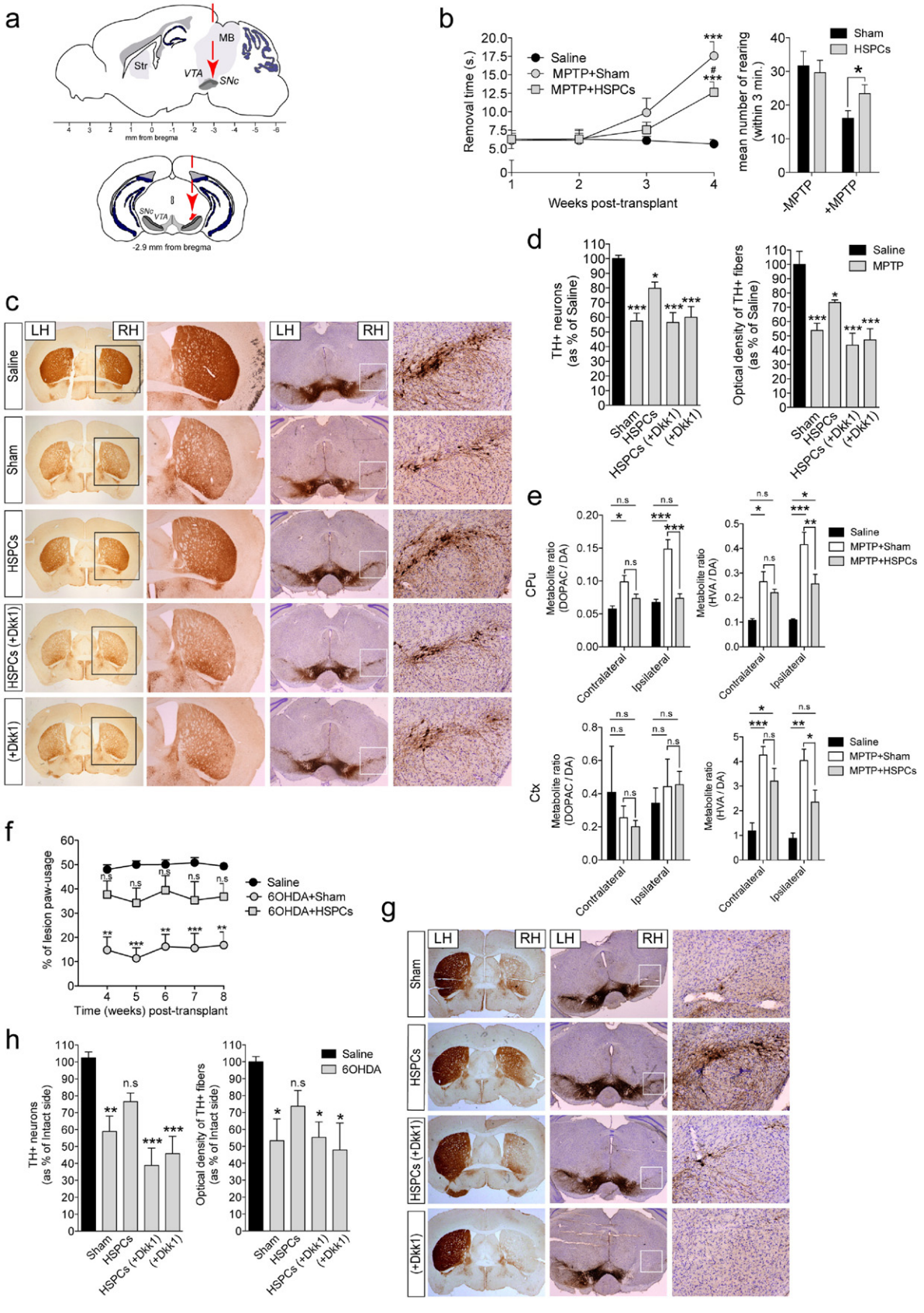

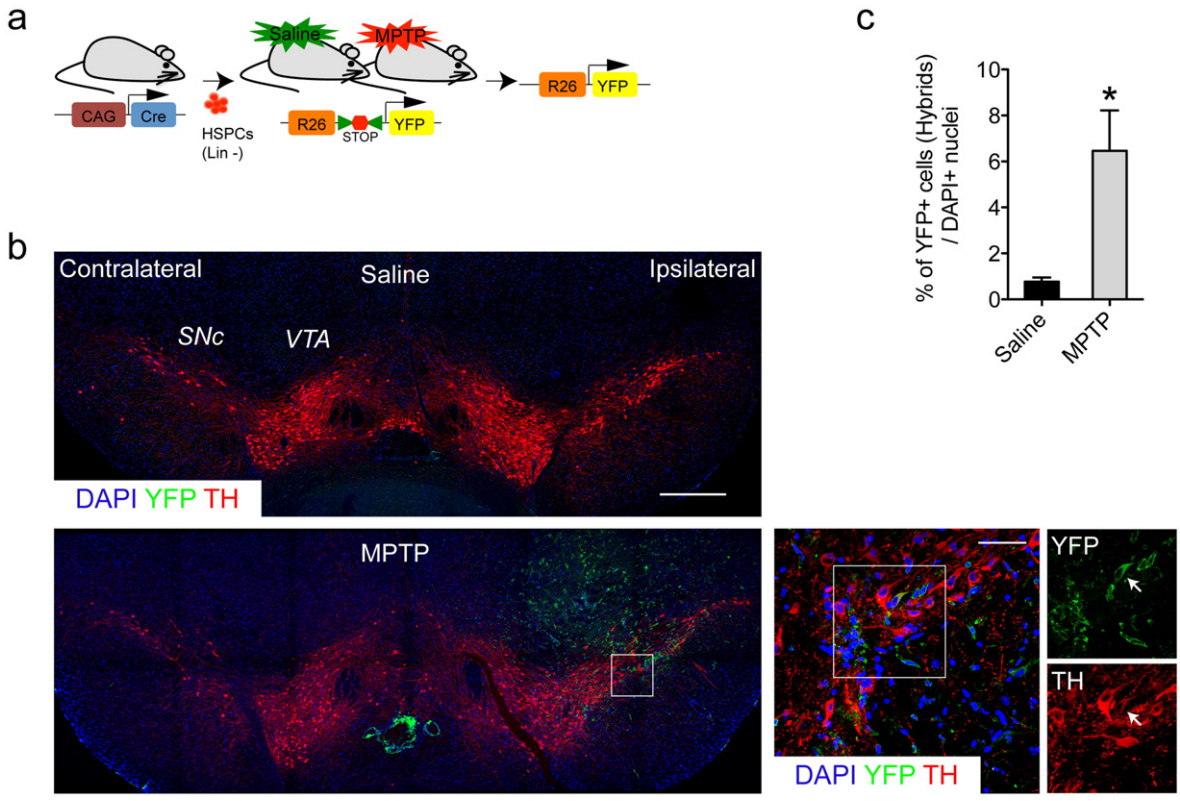

Fig. 2. Hematopoietic stem and progenitor cells spontaneously fuse with brain somatic cells *in vivo*. (a) Outline of the experimental design to detect cell-fusion events. Hybrids were detected by the Cre/loxP system, where Cre-recombinase is under the control of the CAG promoter. Mice were transplanted with lineage-depleted (Lin-) HSPCs after saline and MPTP treatment. Cre-mediated excision of the Stop codon in floxed-loxP transgenic mouse (R26Y), allowing yellow fluorescent protein (YFP) expression. (b) Representative coronal immunostaining sections of adult mouse midbrain showing tyrosine hydroxylase (TH, red) and yellow fluorescent protein (YFP, green) immunopositive cells from the saline and MPTP-treated mice. Cell nuclei were counterstained with DAPI (blue). Contralateral (nongrafted) and ipsilateral (grafted) sites are indicated. Scale bar: 400 μm. Representative higher magnification images are as indicated for the white boxes. TH and YFP immunostaining revealed the double-positive cells (arrows). Scale bar: 50 μm. (c) Quantification of the YFP-immunopositive cells found per DAPI+ nucleus in the saline and MPTP-treated mice. Data are means ± s.e.m (5 sections/mouse; $n = 6$). Statistical analysis is based on Student's *t*-tests. $^{*}P < 0.05$.

obtained in the MPTP model, strongly suggest that intracerebral HSPC transplantation after damage promotes the survival of the endogenous dopaminergic neurons in the SNpc.

3.2. HSPCs Transplanted Above the SNpc can Fuse with Neurons and Glial Cells

We have previously shown that transplanted HSPCs can fuse with retinal neurons (Sanges et al., 2013), and thus we aimed here to also determine the occurrence of fusion events in the SNpc. HSPCs purified from donor mice expressing Cre recombinase under the CAG promoter ($HSPCs^{Cre}$) were unilaterally transplanted above the right SNpc of Rosa26-LoxP-Stop-LoxP-YFP (R26Y) transgenic mice (Fig. 2a, Fig. S2a). Shortly after transplantation, the fusion events, *i.e.*, the hybrids detected by yellow fluorescent protein expression (YFP+), were found in the SNpc and not in the contralateral non-grafted hemisphere. These YFP+ cells were scattered in the ventral midbrain 24 h after transplantation, and some of them were also positive for the dopaminergic neuron marker tyrosine hydroxylase (*i.e.*, TH+) (Fig. 2b, right zooms). The MPTP damage greatly increased the fusion of the transplanted cells (Fig. 2c, Fig. S2a).

A marked inflammatory response induced reduction of the hybrids by 7 days after transplantation (Fig. S2b). An increased density of glial fibrillary acidic protein (GFAP)-positive astroglia delineated the graft (Fig. S2c), which was positively immunostained for the microglia/macrophage marker CD11b, and for the activated microglia marker CD68 (Fig. S2c). Corresponding regions in the contralateral hemisphere and in the sham controls showed glial cell accumulation due to the MPTP-induced damage, or to both MPTP and the needle insertion, respectively (Fig. S2d, e).

Fig. 1. HSPC transplantation functionally rescued dopaminergic neurons. (a) Representation of a sagittal brain section and a coronal section, indicating the site of HSPC transplantation. Midbrain area (MB), substantia nigra pars compacta (SNpc), ventral tegmental area (VTA), and striatum (Str). (b) MPTP + Sham ($n = 8$) and MPTP + HSPCs ($n = 11$) transplanted mice were evaluated for time to stimulus removal (from 1 to 4 weeks after transplantation) and for spontaneous activity upon quantification of the number of rears (4 weeks after transplantation). (c) Representative coronal sections of each group of mice (MPTP model) showing immunohistochemistry of endogenous tyrosine hydroxylase (TH) in the striatum and midbrain. (d) Quantification of the number of TH+ neurons in the midbrain by stereology, and TH+ striatal fibers by optical densitometry, in MPTP + Sham ($n = 11$), MPTP + HSPCs ($n = 11$), MPTP + HSPCs (Dkk1) ($n = 7$), and MPTP + Dkk1 ($n = 7$) transplanted mice, relative to Saline ($n = 8$) transplanted mice. (e) Striatal DA turnover, as determined by the DOPAC/DA and HVA/DA ratios. DA, dopamine; CPu, striatum/caudate-putamen; Ctx, cortex. (f) 6OHDA + Sham ($n = 6$) and 6OHDA + HSPCs ($n = 10$) transplanted mice were assessed for forepaw akinesia using the cylinder test. (g) Representative coronal sections showing TH immunohistochemical labeling for each group of mice (6OHDA model). (h) Percentage of TH+ neurons and fibers loss in the 6OHDA + Sham ($n = 9$), 6OHDA + HSPCs ($n = 10$), 6OHDA + HSPCs (Dkk1) ($n = 8$) and 6OHDA + Dkk1 ($n = 7$) transplanted mice, relative to intact (Saline) side. RH, Right hemisphere; LH, left hemisphere. Data are means ± s.e.m. Statistical analysis is based on one-way ANOVA followed by Bonferroni's multiple comparison *post-hoc* tests. $^{*}P < 0.05$; $^{**}P < 0.01$; $^{***}P < 0.001$ compared with Saline; n.s, not significant; s, seconds.

We next studied the identity of the fusion partners in the hybrids in the midbrain. Most of the YFP+ cells co-expressed the neuronal nucleus protein (NeuN). A small percentage co-expressed GFAP, or the macrophage/microglia marker CD11b. None of the YFP+ cells co-expressed the oligodendrocyte marker (CNPase) (Fig. 3a, b). Thus, the majority of the HSPCs can fuse with neurons and some with glial

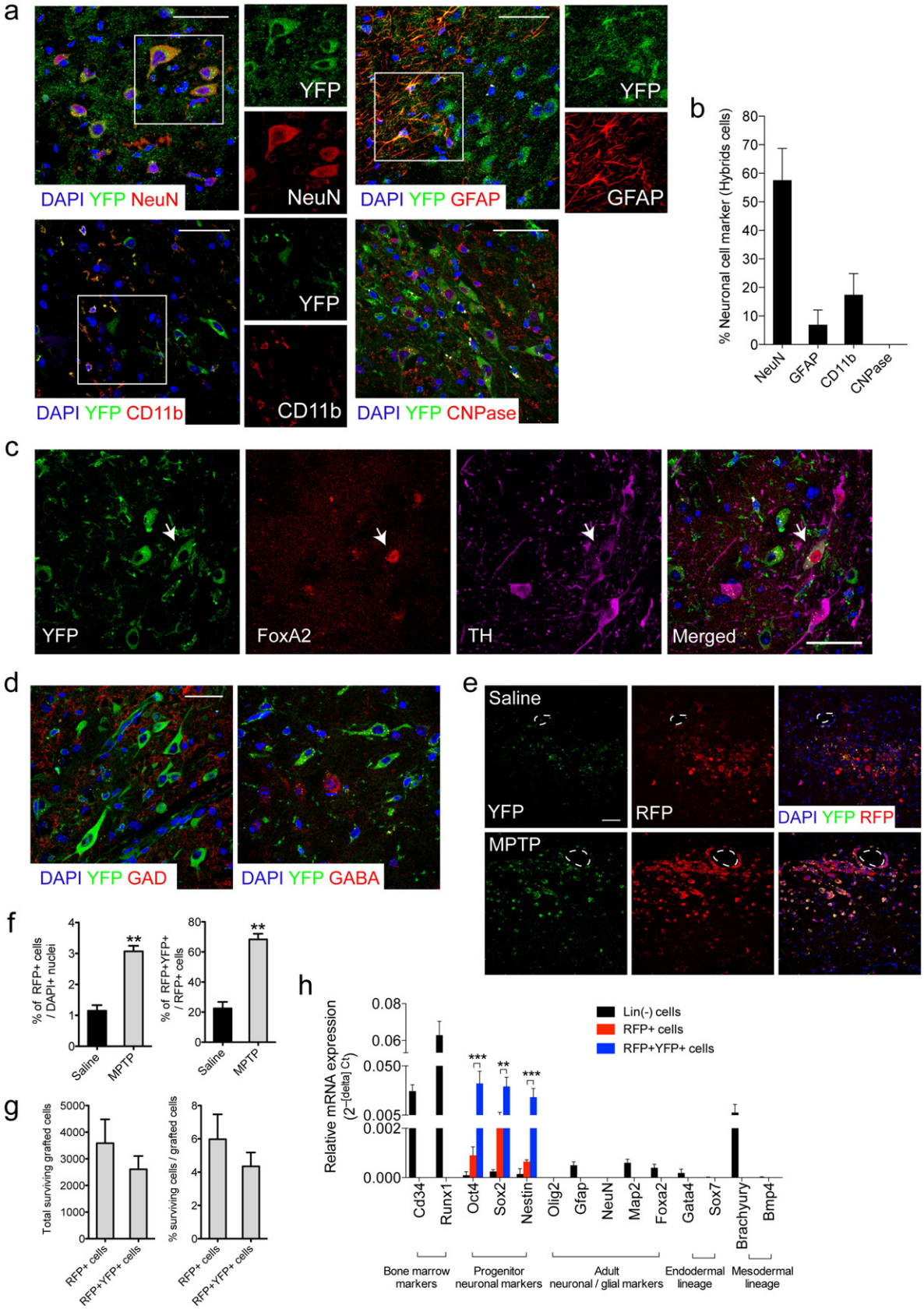

cells. Interestingly, some YFP+ cells in the SNpc co-localized with the ventral midbrain transcription factor (FoxA2) and with TH, both of which are markers of dopaminergic neurons (Fig. 3c). TH is down-regulated after MPTP administration (Jackson-Lewis et al., 1995), and therefore we might have underestimated the number of YFP+TH+, double-positive, cells. In contrast, the YFP+ cells never co-localized with the GABAergic neuron markers γ-aminobutyric acid (GABA) and glutamic acid decarboxylase (GAD) (Fig. 3d).

3.3. Hybrids Undergo Reprogramming In Vivo One Week After HSPC Transplantation

We next analyzed the presence of the hybrids at different times after the transplantation. HSPCs$^{Cre/RFP}$ (isolated from mice carrying β-Actin-Cre and the CAG-RFP alleles) were unilaterally grafted at day 3 after the last MPTP intraperitoneal injection in R26Y mice (Fig. S3a), which corresponds to the peak of apoptotic cell death in this model (Vila et al., 2001). Control mice (injected with saline instead of MPTP) were also grafted. One week after transplantation, there were high numbers of RFP+YFP+ hybrids (Fig. 3e) with round and oval morphologies in the MPTP-treated mice, which were higher than for the saline-treated group (Fig. 3f). Some hybrids were localized throughout the right ventral midbrain site, close to the SNpc, in the parenchyma, while others showed apparent association with vascular elements (Fig. 3e). As expected, due to the marked inflammatory response (S2b–c), the number of surviving hybrids largely decreased 1 week after transplantation as quantified by flow cytometry (FACS) analysis (Fig. 3g).

The change in morphology of the RFP+YFP+ hybrids indicated a possible reprogramming process (Acquistapace et al., 2011). Therefore we analyzed changes in the transcription profiles of the hybrids (RFP+YFP+) and in the unfused RFP+ cells purified from the ventral midbrain (Fig. S3b). In both cell populations, there was almost no expression of adult astroglial or neuronal gene markers (*e.g.*, Gfap, NeuN, Olig2, Foxa2, Map2), and down-regulation of the HSPC markers Cd34 and Runx1. Interestingly, there was higher activation of the pluripotent gene Oct4 in these RFP+YFP+ hybrids, as well as of neuronal precursor genes, such as Sox2 and Nestin, with respect to that observed in the unfused (RFP+) cells (Fig. 3h). In contrast, endoderm and mesoderm lineage markers were not up-regulated in the RFP+YFP+ cells, which overall suggests that the hybrids commit toward neuroectoderm differentiation (Fig. 3h).

Next, to further investigate the reprogrammed phenotype of the hybrids genome-wide, we analyzed the transcriptome of the RFP+YFP+ cells compared to the RFP+ unfused cells using microarrays. A large number of genes were up-regulated in the RFP+YFP+ hybrids with respect to the RFP+ cells (Table S1). Gene ontology (GO) analysis of the up-regulated genes showed a statistically significant enrichment of genes associated with the GO term tissue morphogenesis only in the hybrids (Fig. S3c; Table S2). Overexpression of this set of genes is indicative of a reprogramming process and is in line with the emerging concept of *in vivo* neuronal reprogramming (Amamoto and Arlotta, 2014). Furthermore, gene-set enrichment analysis (Subramanian et al., 2005) showed that hematopoietic stem and progenitor genes were significantly down-regulated in the RFP+YFP+ hybrids (False discovery rate; FDR < 25%), while neurogenesis genes were enriched (Fig. S3d), further indicating reprogramming toward a neuronal lineage.

Overall these data showed that the hybrids that formed *in vivo* undergo reprogramming and morphological changes by 1 week after HSPC transplantation.

3.4. Hybrids Acquire Astroglia Features and Survive Over the Long-term After Transplantation

Four weeks after the intracerebral transplantation, in the MPTP-treated mice, RFP+YFP+ cells located in the ventral midbrain near the SNpc exhibited a morphology typical of glial cells (Fig. 4a). They did not participate in scar formation, as they were not located in the needle track nor in the transplantation site (Fig. S4a). These glial cells showed highly branched fine processes that often contacted the basement membrane that surrounds blood vessels. In the MPTP-treated mice, there were more RFP+ cells than in the Saline-treated mice, and 4.75 ± 1.61% of the RFP+ cells were also YFP+ (Fig. 4b, Fig. S4b). Glial cells that are positive only for RFP suggest possible transdifferentiation from the unfused HSPC-transplanted cells, or silencing of the YFP transgene in the hybrids. Furthermore, we also observed a few YFP+ (RFP-) cells, which were probably hybrids that had switched off the RFP transgene (Fig. 4a).

Most of the RFP+ and YFP+ cells partially co-expressed the astroglial marker GFAP (Fig. 4c). None of the highly branched RFP+ and YFP+ cells co-expressed the microglial marker CD11b or the neuronal marker NeuN (Figure S4c). Nevertheless, we observed some RFP+ cells with a smaller and less-branched shape that showed partial co-localization with CD11b (Figure S4d). Thus, by 4 weeks after transplantation, the RFP+YFP+ cells had mainly acquired properties of mature astroglial cells, and did not express neuronal markers.

We further validated whether the hybrids after fusion of HSPCs with glial cells acquired features of mature astroglia over the long-term. Thus, we grafted HSPCs^{R26Y} into MPTP-treated GFAP-Cre mice, which express Cre only in astroglia (Fig. 4d). Four weeks after transplantation, we observed that YFP+ cells localized in the diseased ventral midbrain associated with GFAP+ astroglial cells (Fig. 4e). Their levels were 5.42 ± 0.38% with respect to the total GFAP+ cell population. Interestingly, this percentage was considerably high considering that after transplantation they were 1.52 ± 0.37% (Fig. 4f). Most of the YFP+ cells co-expressed GFAP (89.75 ± 6.19%) or the mature astrocyte-specific cytosolic protein S100β (Fig. 4g, h). Moreover, some cells also expressed the neuroprogenitor marker Sox2 (Fig. 4i), which suggests that some of the hybrids were reprogrammed. Instead, they did not co-express oligodendrocyte transcription factor 2 (Olig2) or microglia marker Iba-1 (Fig. S4e). There were low levels of YFP-positive cells that were not astroglial cells (10.25% ± 6.19%; Fig. 4h), although we could not identify their nature through marker analysis.

We found GFAP+YFP+ hybrids 4 weeks after transplantation also in the 6OHDA Parkinson's disease model (Fig. S4f). The YFP+ cells co-localized with Cre in the sections from both MPTP- and 6OHDA-transplanted mice, further confirming that the YFP+ cells were indeed hybrids (Fig. S4 g).

Fig. 3. Characterization of hybrids formed *in vivo*. (a–d) R26Y mice transplanted as described in the legend to Fig. 1a were sacrificed 24 h after transplantation ($n = 6$). (a) Representative immunostaining sections of midbrain areas where co-localization of YFP-immunopositive cells with neuronal nuclei protein (NeuN, red), glial fibrillary acid protein (GFAP, red), macrophage/microglia (CD11b), and oligodendrocyte (CNPase) markers are shown. Representative higher magnification zooms from the white boxes are shown. Scale bar: 50 μm. (b) Cell number analysis of the YFP-immunopositive cells showing co-localization with NeuN, GFAP, MAC-1, and CNPase (5 sections/mouse; $n = 6$). (c) Immunostaining showing co-localization of YFP-immunopositive cells with TH (red) and FoxA2 (magenta) at the single-cell level. Arrows indicate co-localization. Scale bar: 50 μm. (d) YFP-immunopositive cells do not co-localize with glutamic acid decarboxylase (GAD, red) and γ-aminobutyric acid (GABA, red). (e-h) MPTP and saline-treated R26Y mice were transplanted as in the legend to Fig. 1a and sacrificed 1 week after transplantation ($n = 4$ each). (e) Representative immunostaining sections from YFP-immunopositive cells co-labeled with red fluorescent protein (RFP, red) in the midbrain of MPTP and saline-treated mice. Some cells showed association with vascular elements (dashed line). Scale bar: 50 μm. (f) (Left) Quantification of the RFP+ cells in the saline and MPTP-treated mice (6 sections/mouse; $n = 4$). (Right) Percentage of the double-positive cells (RFP+YFP+) in the saline and MPTP-treated mice ($n = 4$). (g) (Left) Quantification of FACS-sorted RFP+ and RFP+YFP+ cells from MPTP-treated mice 1 week after transplantation. (Right) Percentage of surviving RFP+ and RFP+YFP+ cells at day 7 post-transplantation calculated with respect to the total transplanted cells (60,000). (h) qRT-PCR analysis of the expression of the indicated genes in the RFP+YFP+ and RFP+ FACS-sorted cells (3 mice/group). In all the immunostaining sections, the cell nuclei were counterstained with DAPI (blue). Data are means ± s.e.m. Statistical analysis is based on Student's *t*-tests. $^{**}P < 0.01$; $^{***}P < 0.001$.

All of these data indicate that only the hybrids derived from the fusion of transplanted HSPCs with glial cells, or the hybrids that acquire astroglia features over the long-term, survive up to 4 weeks after the surgery. To further demonstrate this, we grafted HSPCs^{R26Y} into MPTP-treated FoxA2-Cre mice, to obtain neuron-derived hybrids to follow over the long-term after transplantation (Fig. S4 h). We could not find YFP+ cells with astroglial or neuronal morphologies 4 weeks after transplantation, but only at early time points, further suggesting that neuron-derived hybrids do not survive (Fig. S4i-j). In addition, we FACS-sorted RFP+YFP+ hybrids and RFP+ cells (obtained after

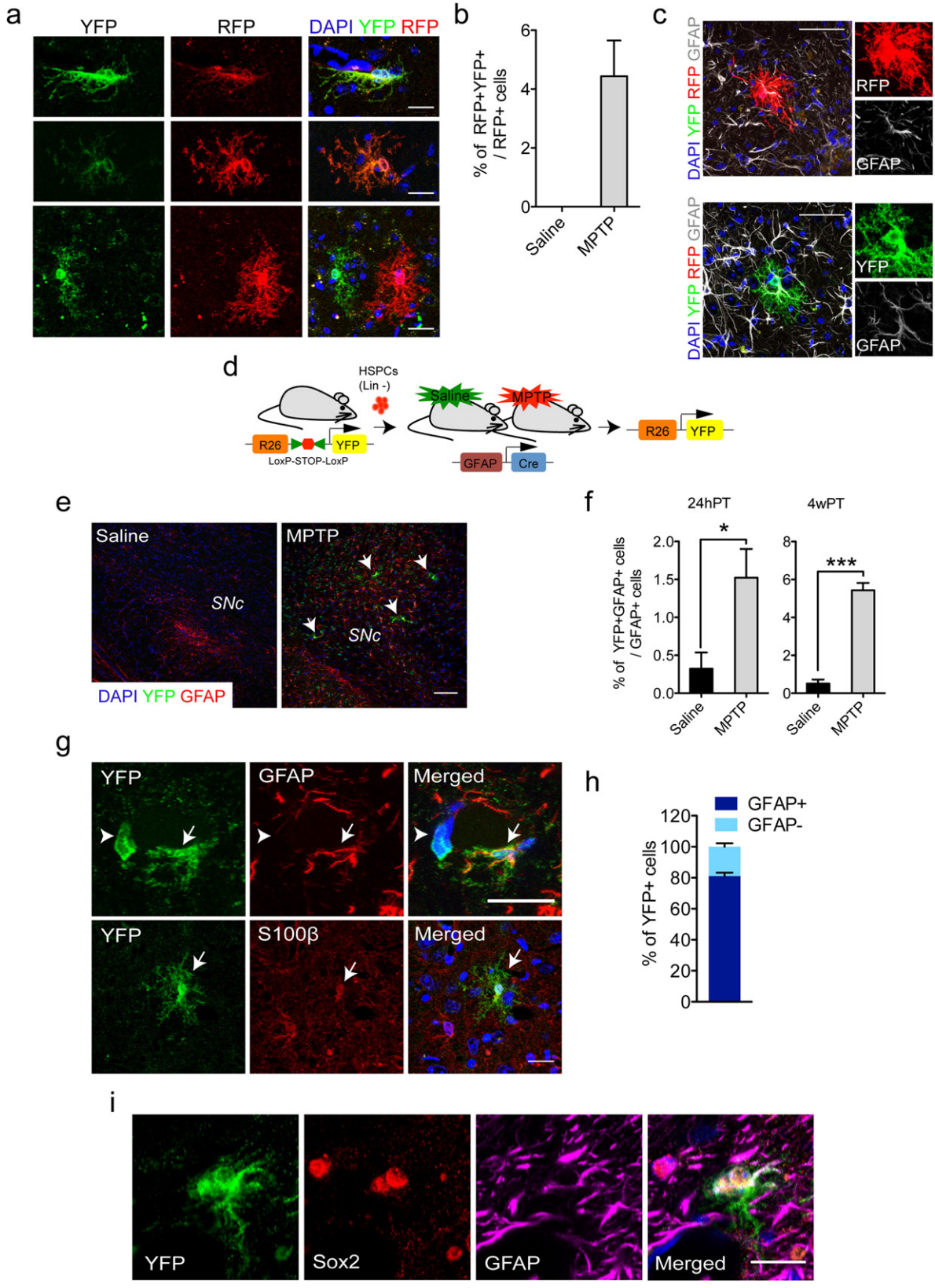

transplanting HSPCs^{R26Y} in MPTP-treated GFAP-Cre or in MPTP-treated FoxA2-Cre mice) and analyzed their transcriptome profile by microarray analysis. Of note, the RFP+YFP+ hybrids obtained from the GFAP-Cre mice were analyzed 7 days after transplantation. Instead the RFP+YFP+ hybrids obtained from the FoxA2-Cre mice were analyzed 5 days after transplantation, as their numbers at 7 days after transplantation were already very low and were not sufficient to perform genome-wide analysis. We performed gene-set enrichment analysis on the up-regulated genes in the hybrids, and we observed that the RFP+YFP+ hybrids obtained from the GFAP-Cre mice were more significantly enriched (FDR < 25%) in neurogenesis genes than those obtained from the FoxA2-Cre mice (Fig. S3e, Tables S3 and S4), further indicating that glial-derived hybrids undergo reprogramming and survive longer. These results are also in agreement with the observation that the RFP+YFP+ hybrids obtained from the R26Y mice display enrichment in neurogenesis genes albeit with high FDR (Fig. S3d), since they include glial- and neuron-derived hybrids. Overall, these data indicate that hybrids formed by HSPCs with neurons appear not to survive over the long-term, as opposed to the glial-derived hybrids.

3.5. Activation of the Wnt Signaling Pathway is Essential for PD Rescue After HSPC Transplantation

The Wnt signaling pathway has a key role in neuronal cell survival and homeostasis (Inestrosa and Arenas, 2010). Moreover, MPTP treatment itself induces temporal and dynamic changes in Wnt signaling components during dopaminergic degeneration (L'episcopo et al., 2010). Consequently, we investigated the changes in Wnt signaling after HSPC transplantation in MPTP-injured mice. We dissected out the ventral midbrain area of transplanted MPTP-treated and saline-treated mice, and observed that the protein levels of the transcriptionally active form of β-catenin underwent significant up-regulation in HSPC-transplanted mice when the lesion was stabilized (Vila et al., 2001) (Fig. S5a, b). Accordingly, the direct Wnt/β-catenin targets Axin2 and the canonical Wnt pathway receptor Fzd1 were up-regulated (Fig. S5c). In contrast, Wnt5a, which is a regulator of the non-canonical pathway, did not change (Fig. S5c). Interestingly, GFAP mRNA (Fig. S5d) and protein (Fig. S5e, f) also increased, which suggests that activation of astroglial cells in the midbrain of the transplanted mice correlates with activation of Wnt signaling after HSPC transplantation. Finally, we observed reduced levels of Caspase-9 expression in the HSPC-transplanted mice, which was comparable to the level in the Saline group, thus indicating reduced apoptosis in the treated mice (Fig. S5g).

Astroglial cells produce Wnt1 (L'episcopo et al., 2010; Zhang et al., 2015), which has been shown to have a trophic effect on neighboring neurons *in vitro* (L'episcopo et al., 2011). We confirmed secretion of Wnt1 by astroglia *in vivo* along the caudal and rostral aqueduct, which is an area that is enriched in astroglia; the rostral area is closest to the transplantation site in the ventral midbrain (Fig. S5h). Interestingly, Wnt1 was internalized by the nearby neurons (Fig. S5h). With this in mind, we analyzed and observed that glial-derived hybrids also secrete Wnt1 (Fig. 5a), which suggests its protective effect on the surrounding dopaminergic neurons. Wnt1 transcript and protein levels were significantly increased in the ventral midbrain after MPTP administration and HSPC transplantation, with respect to the Saline and Sham controls (Fig. 5b, c, Fig. S5i), which indicates increased Wnt1 secretion, which is probably dependent on the hybrids.

As the presence of hybrid-derived astroglia correlated with the observed functional rescue of PD, and at the same time we observed activation of the Wnt/β-catenin canonical pathway in the transplanted area and secretion of Wnt1 by the hybrids, we aimed to address the effect of the block of Wnt/β-catenin signaling activity in the HSPC-transplanted mice. Remarkably, treatment with the Wnt antagonist Dkk1 (unilateral infusion in the SNpc) impaired the recovery of dopaminergic neurons mediated by HSPCs in both the MPTP and 6OHDA models (Fig. 1c, d, f, g), which suggests that activation of the pathway is essential for the observed rescue phenotype.

As a final demonstration that ablation of the hybrids can impair the rescue, we used transgenic mice carrying the Rosa26-LoxP-STOP-LoxP-DTR (R26-diphtheria toxin receptor) and transplanted these with HSPCs$^{Cre/RFP}$ (Fig. 5d). After fusion, the hybrids expressed both RFP and DTR, making them sensitive to diphtheria toxin (DT) injection; thus, they were selectively ablated (Fig. S5j). Four weeks after transplantation, the percentages of TH+ fibers and TH+ neurons were very low in both the Sham and HSPC-transplanted mice that received the toxin (Fig. 5e, f), which indicates that ablation of the hybrids impairs the observed rescue.

4. Discussion

Current cell-therapy strategies in PD models are based on the transplantation of a variety of different cell types into the striatum with the aim of obtaining DA release (Meyer et al., 2010; Gaillard and Jaber, 2011). Release of DA has been shown to occur directly from grafted neural stem cells obtained after differentiation of human embryonic stem cells (Kang et al., 2014). However, the transplanted cells usually do not integrate into the existing basal ganglia circuit, and they are only likely to function as DA producers (Gaillard and Jaber, 2011). In the present study, we aimed to identify ways to functionally rescue the dopaminergic loss in the physiological context; *i.e.*, in the SNpc.

We and others have previously shown that BM-derived cells can fuse with neurons and glial cells in damaged retina and in different damaged brain areas, with functional correction of disease (Johansson et al., 2008; Sanges et al., 2013). Here, we found fusion of HSPCs with TH+ cells, and not with GABA+ or GAD+ cells. This might be because the MPTP-damaged TH+ neurons can release factors that promote fusion with transplanted HSPCs. The GABA+ and GAD+ neurons are instead not damaged by the MPTP treatment. Interestingly, we found hybrids located well away from the injection site in the PD models, which leads us to speculate that these can migrate upon inflammation-mediated chemo-attraction.

Reprogramming of hybrids and their following differentiation into functional retinal neurons has been observed before (Sanges et al., 2013), which suggests that the hybrids are an important source of new cells in the repair of central nervous system function (Lluis and Cosma, 2010). Furthermore, transient expression of precursor and

Fig. 4. Hybrids can acquire features of GFAP-expressing astroglial cells 4 weeks after transplantation. (a–c) R26Y mice transplanted as described in the legend to Fig. 1a were sacrificed 4 weeks after transplantation ($n = 4$). (a) Representative immunostaining sections of midbrain areas showing YFP+ cells (green) with glial morphology co-labeled with RFP (red). YFP or RFP single-positive cells with glial morphology are also shown. Scale bar: 20 μm. (b) Quantification of RFP+YFP+ cells in the saline and MPTP-treated mice ($n = 4$). (c) YFP+ (green) and RFP+ (red) cells expressing the astroglial cell marker GFAP (magenta). Scale bar: 50 μm. (d) Schematic representation of the transplantation scheme and of mouse strains used in (e–i). Cre recombinase is under the control of the GFAP promoter, allowing identification of astroglial-derived hybrids. Mice were sacrificed 4 weeks after transplantation ($n = 4$). (e) Representative immunostaining sections showing YFP+ cells (green) co-expressing the astroglial marker (GFAP, red). Arrows indicate hybrids. Scale bar: 100 μm. (f) Cell fusion quantified 24 h (24hPT) and 4 weeks (4wPT) post-transplantation as the number of YFP+GFAP+ cells with respect to the total GFAP+ cells (6 sections/mouse; $n = 4$). (g) YFP (green) hybrids co-localize (arrows) with GFAP (red) and S100β (red) markers. Arrowheads indicate YFP+GFAP- cells. Scale bar: 20 μm. (h) Quantification of YFP+GFAP+ and YFP+GFAP- cells. (i) Hybrid reprogramming is shown by triple immunostaining for YFP (green), Sox2 (red), and GFAP (magenta). Scale bar: 20 μm. In all immunostaining images, the cell nuclei were counterstained with DAPI (blue). Data are means ± s.e.m. Statistical analysis is based on Student's *t*-tests. ***$P < 0.001$; n.s: not significant.

pluripotency markers appears to occur in some cases during transdifferentiation or *in vivo* cell fusion (Sanges et al., 2013; Bar-Nur et al., 2015). Whether the transient re-expression of pluripotency genes is a driver for efficient differentiation of the hybrids into the correct lineage still remains to be defined.

Here, we showed that the presence of glial-derived hybrids correlated with the functional rescue of PD. Although the hybrids underwent reprogramming by expressing precursor markers, we did not observe relevant conversion of the hybrids into newly generated dopaminergic neurons. It is possible that other additional signals that were not activated under our experimental conditions are necessary for the hybrids to be eventually differentiated into neurons. Alternatively, timing might also be a critical variable; *i.e.* possible few hybrids committed to differentiation in neurons in the brain might need a long time.

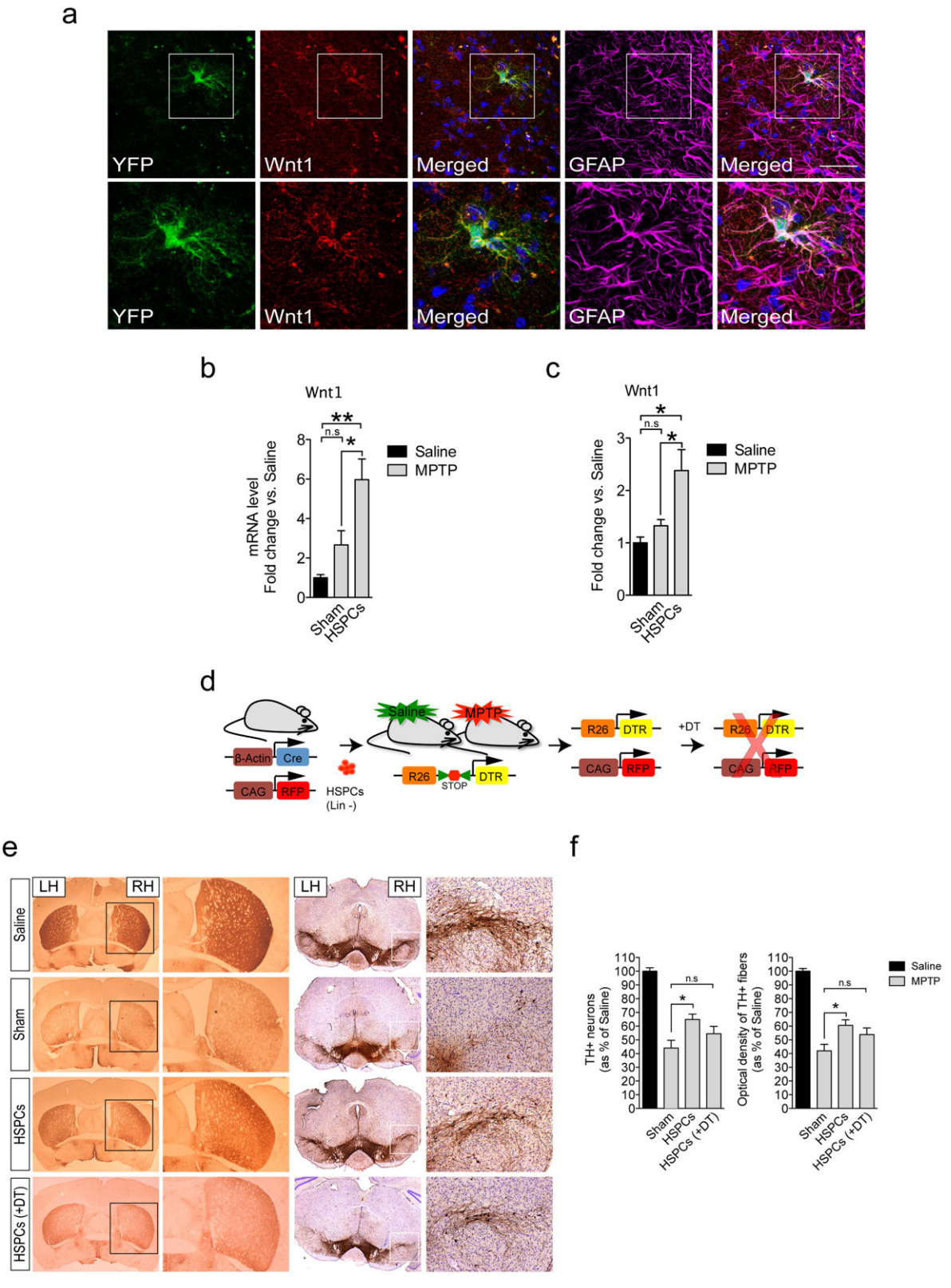

On the other hand, the transplantation of HSPCs appears to induce protection against dopaminergic neuron loss due to a niche-mediated effect of the glial-derived hybrids, which release Wnt1 and perhaps other to-be-identified neurotrophic factors.

Previously, it was shown that the Wnt1 transcript is strongly induced in MPTP-reactive astroglia, and the release of Wnt1 from these cells was suggested (L'episcopo et al., 2010, 2014b; Zhang et al., 2015). Our data show here that Dkk1-mediated blockade of the endogenous Wnt/β-catenin pathway impairs the observed rescue, which suggests that the already high levels of the endogenous Wnt pathway after the MPTP and 6ODHA treatments is sufficient to activate the transplanted HSPCs.

We found that Wnt1 is efficiently secreted from astroglia in the aqueduct of the caudal area in adult mice, and also in the rostral area, which is closest to the area of transplantation in the ventral midbrain. It is known that the activation of canonical Wnt/β-catenin signaling can prevent secretion of pro-inflammatory cytokines from the microglia, and along with the recognized role of astroglia as a source of survival, neurotrophic, and neurogenic factors, this can favor the rescue of DA neurons (L'Episcopo et al., 2014a).

A glial-cell-mediated niche effect might well be a way to protect nigral dopaminergic neurons from neurotoxin-induced cell death. Optogenetically activated astrocytes in the MPTP mouse model were shown to produce basic fibroblast growth factor, which in turn enhanced the dopaminergic differentiation of transplanted human embryonic stem cells, and also protected against dopaminergic neuron loss (Yang et al., 2014). Overall, dopaminergic neuron plasticity and survival can be sustained by trophic factors released by nearby astroglial cells, which might become an important target for PD therapy (Marchetti et al., 2013).

In our cell-therapy approach, although we observed a significant amelioration of the dopaminergic neuron loss, there was also a drastic decrease in the hybrids already 1 week after transplantation. This was due to the immune response against the graft. In the future if a way to enhance the survival of the hybrids can be identified, it is likely that the observed functional rescue will be much increased. Also the ectopic activation of the Wnt pathway in the transplanted cells or directly at the site of transplantation might be beneficial in aged mice, where it has been shown that the damage-dependent activation of the pathway is not so relevant (L'episcopo et al., 2010). Along with Wnt signaling activation, the use of molecules that can enhance differentiation of the hybrids, such as brain-derived neurotrophic factor (BDNF) and glial cell-derived neurotrophic factor (GDNF) (Deierborg et al., 2008; Enciu et al., 2011) might also be beneficial for improving the rescue of the PD phenotype.

Unilateral transplantation of HSPCs in the bilateral MPTP-damaged mice resulted in a greater number of surviving TH+ neurons ipsilateral to the graft, compared to animals transplanted with PBS (*i.e.*, the Sham group). On the other hand, the transplantation of one side can also be propagated to the other side, as the GFAP-derived hybrids secrete neurotrophic factors, and these can diffuse through both hemispheres and rescue the defects bilaterally (Sieber-Blum, 2010). Previous published data have shown rescue of contralateral non-transplanted sites in the MPTP mouse model (Ourednik et al., 2002, 2009). Indeed, we observed a tendency (although, as expected, it did not reach significance) for the rescue of the non-transplanted hemisphere at the level of both the fibers and the cell bodies. This was also evident (although only as a trend) when we measured the metabolite to DA ratio in the contralateral side, both in the cortex and the striatum.

Overall, our data here suggest that our approach can be efficient for the rescue of both hemispheres; however to increase efficacy, several clinical trials have reported that bilateral transplantation might be necessary (Peschanski et al., 1994; Defer et al., 1996; Venkataramana et al., 2010, 2012).

In conclusion, our data show that reprogramming of HSPC-derived hybrids and their acquisition of mature astroglial features indicate fusion-mediated plasticity of adult neural cells *in vivo*. HSPC-mediated fusion appears to be an efficient approach to prevent neuronal loss and to rescue neurobehavioral function in PD. Importantly, HSPCs are already used in the clinic (Deda et al., 2009; Chen et al., 2014a, 2014b; Park et al., 2015), which suggests their safety, and therefore this cell-therapy method might be translated into the clinic smoothly.

Supplementary data to this article can be found online at http://dx.doi.org/10.1016/j.ebiom.2016.04.016.

Funding Sources

We are grateful for the support from a Fundació La Marató de TV3 grant (120530 to M.P.C. and M.V.), an ERC grant (242630-RERE to M.P.C.), Ministerio de Ciencia e Inovación grants (SAF2011-28580, 2014SGR1137 and BFU2015-71984-ERC to M.P.C.), an AGAUR grant (2014 SGR 780 to M.P.C.), Fondo de Investigación Sanitaria-Instituto de Salud Carlos III grants (PI13/01897 to M.V.; CP11/00229 to J.B.), an AGAUR-GRC grant (2014-SGR-1609 to M.V.), European Union Seventh Framework Programme (FP7/2007-2013) under the Marie Curie Intra-European Fellowship (274882 to W.A.X) and Juan de la Cierva fellowship (to W.A.X), Spanish Ministry of Economy and Competitiveness, 'Centro de Excelencia Severo Ochoa 2013-2017', SEV-2012-0208.

Author Contributions

W.A.X. designed and performed the experiments, interpreted the data, and wrote the manuscript. U.d.V helped with animal handling, surgery and contributes to some of the experiments. M.M.M helped with animal handling. J.B performed some experiments related to MPTP intoxication and transplantation and assisted in their interpretation. A.B. carried out DA and metabolites biochemical quantifications and interpreted the results. M.V. assisted with the design and interpretation of the experiments. M.P.C. oversaw, designed, interpreted experiments and data, and wrote the manuscript.

Conflict of interest

The authors declare no competing financial interests.

Acknowledgments

The authors thank Karthik Arumugam, Francesco Aulicino, Frederic Lluis Viñas, Lucia Marucci, Neus Romo, Elisa Pedone, Stefano Pluchino and Daniela Sanges for the suggestions and critical reading of the

Fig. 5. Newly generated hybrid-derived astroglia secrete Wnt1. (a) Wnt1 protein (red) co-localization with YFP+ hybrids (green) and the astroglia marker GFAP (magenta) in GFAP-cre transplanted mice sacrificed 4 weeks after transplantation. Scale bar: 50 μm. Representative higher magnification images are as indicated for the white boxes. In all immunostaining images, cell nuclei were counterstained with DAPI (blue). (b, c) Quantification of Wnt1 mRNA (b) and protein (c) levels in midbrain homogenates of transplanted mice. The housekeeping gene and protein, β-Actin, was used to normalize the qRT-PCR and Western blotting, respectively. Data are means ± s.e.m. for fold changes *versus* Saline mice, ($n = 4$–6/group). Statistical analysis is based on one-way ANOVA followed by Bonferroni's multiple comparison *post-hoc* tests. $^{*}P < 0.05$; $^{**}P < 0.01$; n.s: not significant. (d) R26iDTR mice transplanted as described in the legend to Fig. 1a were sacrificed 4 weeks after transplantation. (e) Representative coronal sections of each group of mice (MPTP model) showing immunohistochemistry of endogenous TH in the striatum and midbrain. (f) Quantification of the number of TH+ neurons in the midbrain by stereology, and TH+ striatal fibers by optical densitometry, in MPTP + Sham ($n = 9$), MPTP + HSPCs ($n = 10$) and MPTP + HSPCs (DT) ($n = 9$) mice relative to Saline ($n = 6$) mice. DT, diphtheria toxin; RH, right hemisphere; LH, left hemisphere. Data are means ± s.e.m. Statistical analysis is based on one-way ANOVA followed by Bonferroni's multiple comparison *post-hoc* tests. $^{*}P < 0.05$ compared to Sham; n.s, not significant.

manuscript; Eduardo Fernandez and Cristina Soto for the help with behavioral tests; Annabelle Parent for the help with the mouse-brain cryo-sectioning; Sarah Bonnin for the help with the bioinformatics analysis; Esther Ruiz-Bronchal and Letizia Campa for the technical assistance of HPLC; Histology, FACS, bioinformatics and Microscopy CRG Facilities and PRBB Animal Facility.

References

Acquistapace, A., Bru, T., Lesault, P.F., Figeac, F., Coudert, A.E., le Coz, O., Christov, C., Baudin, X., Auber, F., et al., 2011. Human mesenchymal stem cells reprogram adult cardiomyocytes toward a progenitor-like state through partial cell fusion and mitochondria transfer. Stem Cells 29, 812–824.

Amamoto, R., Arlotta, P., 2014. Development-inspired reprogramming of the mammalian central nervous system. Science 343, 1239882.

Bar-Nur, O., Verheul, C., Sommer, A.G., Brumbaugh, J., Schwarz, B.A., Lipchina, I., Huebner, A.J., Mostoslavsky, G., Hochedlinger, K., 2015. Lineage conversion induced by pluripotency factors involves transient passage through an iPSC stage. Nat. Biotechnol. 33, 761–768.

Bortolozzi, A., Artigas, F., 2003. Control of 5-hydroxytryptamine release in the dorsal raphe nucleus by the noradrenergic system in rat brain. Role of alpha-adrenoceptors. Neuropsychopharmacology 28, 421–434.

Bové, J., Perier, C., 2012. Neurotoxin-based models of Parkinson's disease. Neuroscience 211, 51–76.

Buch, T., Heppner, F.L., Tertilt, C., Heinen, T.J., Kremer, M., Wunderlich, F.T., Jung, S., Waisman, A., 2005a. A Cre-inducible diphtheria toxin receptor mediates cell lineage ablation after toxin administration. Nat. Methods 2, 419–426.

Buch, T., Heppner, F.L., Tertilt, C., Heinen, T.J., Kremer, M., Wunderlich, F.T., Jung, S., Waisman, A., 2005b. A Cre-inducible diphtheria toxin receptor mediates cell lineage ablation after toxin administration. Nat. Methods 2, 419–426.

Chen, D.C., Lin, S.Z., Fan, J.R., Lin, C.H., Lee, W., Lin, C.C., Liu, Y.J., Tsai, C.H., Chen, J.C., et al., 2014a. Intracerebral implantation of autologous peripheral blood stem cells in stroke patients: a randomized phase II study. Cell Transplant. 23, 1599–1612.

Chen, D.C., Lin, S.Z., Fan, J.R., Lin, C.H., Lee, W., Lin, C.C., Liu, Y.J., Tsai, C.H., Chen, J.C., et al., 2014b. Intracerebral implantation of autologous peripheral blood stem cells in stroke patients: a randomized phase II study. Cell Transplant. 23, 1599–1612.

Decressac, M., Mattsson, B., Lundblad, M., Weikop, P., Björklund, A., 2012. Progressive neurodegenerative and behavioural changes induced by AAV-mediated overexpression of α-synuclein in midbrain dopamine neurons. Neurobiol. Dis. 45, 939–953.

Deda, H., Inci, M.C., Kürekçi, A.E., Sav, A., Kayihan, K., Ozgün, E., Ustünsoy, G.E., Kocabay, S., 2009. Treatment of amyotrophic lateral sclerosis patients by autologous bone marrow-derived hematopoietic stem cell transplantation: a 1-year follow-up. Cytotherapy 11, 18–25.

Defer, G.L., Geny, C., Ricolfi, F., Fenelon, G., Monfort, J.C., Remy, P., Villafane, G., Jeny, R., Samson, Y., et al., 1996. Long-term outcome of unilaterally transplanted parkinsonian patients.I. Clinical approach. Brain 119 (Pt 1), 41–50.

Deierborg, T., Soulet, D., Roybon, L., Hall, V., Brundin, P., 2008. Emerging restorative treatments for Parkinson's disease. Prog. Neurobiol. 85, 407–432.

Doyonnas, R., LaBarge, M.A., Sacco, A., Charlton, C., Blau, H.M., 2004. Hematopoietic contribution to skeletal muscle regeneration by myelomonocytic precursors. Proc. Natl. Acad. Sci. U. S. A. 101, 13507–13512.

Duty, S., Jenner, P., 2011. Animal models of Parkinson's disease: a source of novel treatments and clues to the cause of the disease. Br. J. Pharmacol. 164, 1357–1391.

Enciu, A.M., Nicolescu, M.I., Manole, C.G., Mureşanu, D.F., Popescu, L.M., Popescu, B.O., 2011. Neuroregeneration in neurodegenerative disorders. BMC Neurol. 11, 75.

Fleming, S.M., Ekhator, O.R., Ghisays, V., 2013. Assessment of sensorimotor function in mouse models of Parkinson's disease. J. Vis. Exp. 76. http://dx.doi.org/10.3791/50303.

Gaillard, A., Jaber, M., 2011. Rewiring the brain with cell transplantation in Parkinson's disease. Trends Neurosci. 34, 124–133.

Gregorian, C., Nakashima, J., Le Belle, J., Ohab, J., Kim, R., Liu, A., Smith, K.B., Groszer, M., Garcia, A.D., Sofroniew, M.V., Carmichael, S.T., Kornblum, H.I., Liu, X., Wu, H., 2009. Pten deletion in adult neural stem/progenitor cells enhances constitutive neurogenesis. J. Neurosci. 29, 1874–1886.

Hayashi, S., McMahon, A.P., 2002. Efficient recombination in diverse tissues by a tamoxifen-inducible form of Cre: a tool for temporally regulated gene activation/inactivation in the mouse. Dev. Biol. 244, 305–318.

Inestrosa, N.C., Arenas, E., 2010. Emerging roles of Wnts in the adult nervous system. Nat. Rev. Neurosci. 11, 77–86.

Jackson-Lewis, V., Jakowec, M., Burke, R.E., Przedborski, S., 1995. Time course and morphology of dopaminergic neuronal death caused by the neurotoxin 1-methyl-4-phenyl-1,2,3,6-tetrahydropyridine. Neurodegeneration 4, 257–269.

Johansson, C.B., Youssef, S., Koleckar, K., Holbrook, C., Doyonnas, R., Corbel, S.Y., Steinman, L., Rossi, F.M., Blau, H.M., 2008. Extensive fusion of haematopoietic cells with Purkinje neurons in response to chronic inflammation. Nat. Cell Biol. 10, 575–583.

de Jong, J.H., Rodermond, H.M., Zimberlin, C.D., Lascano, V., De Sousa E Melo, F., Richel, D.J., Medema, J.P., Vermeulen, L., 2012. Fusion of intestinal epithelial cells with bone marrow derived cells is dispensable for tissue homeostasis. Sci. Rep. 2, 271.

Kang, X., Xu, H., Teng, S., Zhang, X., Deng, Z., Zhou, L., Zuo, P., Liu, B., Liu, B., et al., 2014. Dopamine release from transplanted neural stem cells in parkinsonian rat striatum in vivo. Proc. Natl. Acad. Sci. U. S. A. 111, 15804–15809.

Keshet, G.I., Tolwani, R.J., Trejo, A., Kraft, P., Doyonnas, R., Clayberger, C., Weimann, J.M., Blau, H.M., 2007. Increased host neuronal survival and motor function in BMT parkinsonian mice: involvement of immunosuppression. J. Comp. Neurol. 504, 690–701.

Kilkenny, C., Browne, W.J., Cuthill, I.C., Emerson, M., Altman, D.G., 2010. Improving bioscience research reporting: the ARRIVE guidelines for reporting animal research. PLoS Biol. 8, e1000412.

L'episcopo, F., Serapide, M.F., Tirolo, C., Testa, N., Caniglia, S., Morale, M.C., Pluchino, S., Marchetti, B., 2011. A Wnt1 regulated frizzled-1/β-catenin signaling pathway as a candidate regulatory circuit controlling mesencephalic dopaminergic neuron-astrocyte crosstalk: therapeutical relevance for neuron survival and neuroprotection. Mol. Neurodegener. 6, 49.

L'Episcopo, F., Tirolo, C., Caniglia, S., Testa, N., Morale, M.C., Serapide, M.F., Pluchino, S., Marchetti, B., 2014a. Targeting Wnt signaling at the neuroimmune interface for dopaminergic neuroprotection/repair in Parkinson's disease. J. Mol. Cell Biol. 6, 13–26.

L'episcopo, F., Tirolo, C., Testa, N., Caniglia, S., Morale, M.C., Cossetti, C., D'Adamo, P., Zardini, E., Andreoni, L., Ihekwaba, A.E., Serra, P.A., Franciotta, D., Martino, G., Pluchino, S., Marchetti, B., 2010. Reactive astrocytes and Wnt/β-catenin signaling link nigrostriatal injury to repair in 1-methyl-4-phenyl-1,2,3,6-tetrahydropyridine model of Parkinson's disease. Neurobiol. Dis. 41 (2), 508–527.

L'episcopo, F., Tirolo, C., Testa, N., Caniglia, S., Morale, M.C., Serapide, M.F., Pluchino, S., Marchetti, B., 2014b. Wnt/β-catenin signaling is required to rescue midbrain dopaminergic progenitors and promote neurorepair in ageing mouse model of Parkinson's disease. Stem Cells 32, 2147–2163.

Lluis, F., Cosma, M.P., 2010. Cell-fusion-mediated somatic-cell reprogramming: a mechanism for tissue regeneration. J. Cell. Physiol. 223 (1), 6–13.

Long, J.Z., Lackan, C.S., Hadjantonakis, A.K., 2005. Genetic and spectrally distinct in vivo imaging: embryonic stem cells and mice with widespread expression of a monomeric red fluorescent protein. BMC Biotechnol. 5, 20.

Marchetti, B., L'Episcopo, F., Morale, M.C., Tirolo, C., Testa, N., Caniglia, S., Serapide, M.F., Pluchino, S., 2013. Uncovering novel actors in astrocyte-neuron crosstalk in Parkinson's disease: the Wnt/β-catenin signaling cascade as the common final pathway for neuroprotection and self-repair. Eur. J. Neurosci. 37, 1550–1563.

Meredith, G.E., Kang, U.J., 2006. Behavioral models of Parkinson's disease in rodents: a new look at an old problem. Mov. Disord. 21, 1595–1606.

Meyer, A.K., Maisel, M., Hermann, A., Stirl, K., Storch, A., 2010. Restorative approaches in Parkinson's disease: which cell type wins the race? J. Neurol. Sci. 289, 93–103.

Nygren, J.M., Jovinge, S., Breitbach, M., Säwén, P., Röll, W., Hescheler, J., Taneera, J., Fleischmann, B.K., Jacobsen, S.E., 2004. Bone marrow-derived hematopoietic cells generate cardiomyocytes at a low frequency through cell fusion, but not transdifferentiation. Nat. Med. 10, 494–501.

Ogle, B.M., Cascalho, M., Platt, J.L., 2005. Biological implications of cell fusion. Nat. Rev. Mol. Cell Biol. 6, 567–575.

Ourednik, J., Ourednik, V., Lynch, W.P., Schachner, M., Snyder, E.Y., 2002. Neural stem cells display an inherent mechanism for rescuing dysfunctional neurons. Nat. Biotechnol. 20, 1103–1110.

Ourednik, V., Ourednik, J., Xu, Y., Zhang, Y., Lynch, W.P., Snyder, E.Y., Schachner, M., 2009. Cross-talk between stem cells and the dysfunctional brain is facilitated by manipulating the niche: evidence from an adhesion molecule. Stem Cells 27, 2846–2856.

Parish, C.L., Finkelstein, D.I., Drago, J., Borrelli, E., Horne, M.K., 2001. The role of dopamine receptors in regulating the size of axonal arbors. J. Neurosci. Off. J. Soc. Neurosci. 21 (14), 5147–5157.

Park, E.J., Sun, X., Nichol, P., Saijoh, Y., Martin, J.F., Moon, A.M., 2008. System for tamoxifen-inducible expression of cre-recombinase from the Foxa2 locus in mice. Dev. Dyn. 237, 447–453.

Park, S.S., Bauer, G., Abedi, M., Pontow, S., Panorgias, A., Jonnal, R., Zawadzki, R.J., Werner, J.S., Nolta, J., 2015. Intravitreal autologous bone marrow CD34+ cell therapy for ischemic and degenerative retinal disorders: preliminary phase 1 clinical trial findings. Invest. Ophthalmol. Vis. Sci. 56, 81–89.

Paxinos, G., Franklin, K.B.J., 2008. The Mouse Brain in Stereotaxic Coordinates, Compact. third ed. Elsevier Academic Press, New York.

Peschanski, M., Defer, G., N'Guyen, J.P., Ricolfi, F., Monfort, J.C., Remy, P., Geny, C., Samson, Y., Hantraye, P., Jeny, R., 1994. Bilateral motor improvement and alteration of L-dopa effect in two patients with Parkinson's disease following intrastriatal transplantation of foetal ventral mesencephalon. Brain 117 (Pt 3), 487–499.

de Rijk, M.C., Tzourio, C., Breteler, M.M., Dartigues, J.F., Amaducci, L., Lopez-Pousa, S., Manubens-Bertran, J.M., Alpérovitch, A., Rocca, W.A., 1997. Prevalence of parkinsonism and Parkinson's disease in Europe: the EUROPARKINSON Collaborative Study. European community concerted action on the epidemiology of Parkinson's disease. J. Neurol. Neurosurg. Psychiatry 62, 10–15.

Sanges, D., Romo, N., Simonte, G., Di Vicino, U., Diaz Tahoces, A., Fernández, E., Cosma, M.P., 2013. Wnt/b-Catenin Signaling Triggers Neuron Reprogramming and Regeneration in the Mouse Retina. Cell Rep 4, 1–16.

Schallert, T., Fleming, S.M., Leasure, J.L., Tillerson, J.L., Bland, S.T., 2000. CNS plasticity and assessment of forelimb sensorimotor outcome in unilateral rat models of stroke, cortical ablation, parkinsonism and spinal cord injury. Neuropharmacology 39, 777–787.

Sieber-Blum, M., 2010. Epidermal neural crest stem cells and their use in mouse models of spinal cord injury. Brain Res. Bull. 83, 189–193.

Srinivas, S., Watanabe, T., Lin, C.S., William, C.M., Tanabe, Y., Jessell, T.M., Costantini, F., 2001. Cre reporter strains produced by targeted insertion of EYFP and ECFP into the ROSA26 locus. BMC Dev. Biol. 1, 4.

Subramanian, A., Tamayo, P., Mootha, V.K., Mukherjee, S., Ebert, B.L., Gillette, M.A., Paulovich, A., Pomeroy, S.L., Golub, T.R., et al., 2005. Gene set enrichment analysis: a

knowledge-based approach for interpreting genome-wide expression profiles. Proc. Natl. Acad. Sci. U. S. A. 102, 15545–15550.

Venkataramana, N.K., Kumar, S.K., Balaraju, S., Radhakrishnan, R.C., Bansal, A., Dixit, A., Rao, D.K., Das, M., Jan, M., et al., 2010. Open-labeled study of unilateral autologous bone-marrow-derived mesenchymal stem cell transplantation in Parkinson's disease. Transl. Res. 155, 62–70.

Venkataramana, N.K., Pal, R., Rao, S.A., Naik, A.L., Jan, M., Nair, R., Sanjeev, C.C., Kamble, R.B., Murthy, D.P., Chaitanya, K., 2012. Bilateral transplantation of allogenic adult human bone marrow-derived mesenchymal stem cells into the subventricular zone of Parkinson's disease: a pilot clinical study. Stem Cells Int. 2012, 931902.

Vila, M., Jackson-Lewis, V., Vukosavic, S., Djaldetti, R., Liberatore, G., Offen, D., Korsmeyer, S.J., Przedborski, S., 2001. Bax ablation prevents dopaminergic neurodegeneration in the 1-methyl-4-phenyl-1,2,3,6-tetrahydropyridine mouse model of Parkinson's disease. Proc. Natl. Acad. Sci. U. S. A. 98, 2837–2842.

Wang, X., Willenbring, H., Akkari, Y., Torimaru, Y., Foster, M., Al-Dhalimy, M., Lagasse, E., Finegold, M., Olson, S., Grompe, M., 2003. Cell fusion is the principal source of bone-marrow-derived hepatocytes. Nature 422, 897–901.

Yang, F., Liu, Y., Tu, J., Wan, J., Zhang, J., Wu, B., Chen, S., Zhou, J., Mu, Y., Wang, L., 2014. Activated astrocytes enhance the dopaminergic differentiation of stem cells and promote brain repair through bFGF. Nat. Commun. 5, 5627.

Zhang, J., Götz, S., Vogt Weisenhorn, D.M., Simeone, A., Wurst, W., Prakash, N., 2015. A WNT1-regulated developmental gene cascade prevents dopaminergic neurodegeneration in adult En1 (±) mice. Neurobiol. Dis. 82, 32–45.